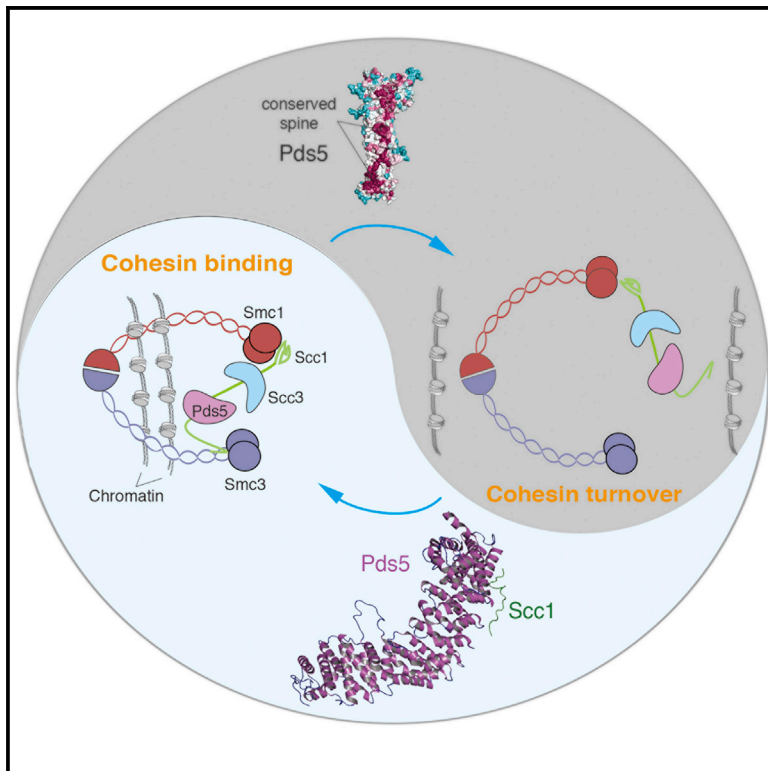


## Structure of the Pds5-Scc1 Complex and Implications for Cohesin Function

### Graphical Abstract



### Authors

Kyle W. Muir, Marc Kschonsak, Yan Li, Jutta Metz, Christian H. Haering, Daniel Panne

### Correspondence

panne@embl.fr

### In Brief

Pds5 regulates the stability with which cohesin engages chromatin and pairs chromosomes. Muir et al. present structural insight into the molecular basis of Pds5 function and recruitment to cohesin. Structure-guided mutagenesis reveals a direct correlation between the strength of Pds5-cohesin binding, maintenance of sister chromatid cohesion, and cell viability.

### Highlights

- The structure of Pds5 reveals conserved surface features in the HEAT repeat domain
- Pds5 interacts with a discrete binding module on Scc1
- Enduring sister chromatid cohesion requires robust Pds5-Scc1 interactions
- A conserved surface spine in the Pds5 N terminus may contribute to cohesin release

### Accession Numbers

5frp  
5frr  
5frs



# Structure of the Pds5-Scc1 Complex and Implications for Cohesin Function

Kyle W. Muir,<sup>1</sup> Marc Kschonsak,<sup>2</sup> Yan Li,<sup>1</sup> Jutta Metz,<sup>2</sup> Christian H. Haering,<sup>2</sup> and Daniel Panne<sup>1,\*</sup>

<sup>1</sup>European Molecular Biology Laboratory Grenoble Outstation and Unit of Virus Host-Cell Interactions, University Grenoble Alpes-CNRS-EMBL, 71 Avenue des Martyrs, CS 90181, 38042 Grenoble Cedex 9, France

<sup>2</sup>European Molecular Biology Laboratory, Cell Biology and Biophysics Unit and Structural and Computational Biology Unit, Meyerhofstrasse 1, 69117 Heidelberg, Germany

\*Correspondence: [panne@embl.fr](mailto:panne@embl.fr)

<http://dx.doi.org/10.1016/j.celrep.2016.01.078>

This is an open access article under the CC BY license (<http://creativecommons.org/licenses/by/4.0/>).

## SUMMARY

Sister chromatid cohesion is a fundamental prerequisite to faithful genome segregation. Cohesion is precisely regulated by accessory factors that modulate the stability with which the cohesin complex embraces chromosomes. One of these factors, Pds5, engages cohesin through Scc1 and is both a facilitator of cohesion, and, conversely also mediates the release of cohesin from chromatin. We present here the crystal structure of a complex between budding yeast Pds5 and Scc1, thus elucidating the molecular basis of Pds5 function. Pds5 forms an elongated HEAT repeat that binds to Scc1 via a conserved surface patch. We demonstrate that the integrity of the Pds5-Scc1 interface is indispensable for the recruitment of Pds5 to cohesin, and that its abrogation results in loss of sister chromatid cohesion and cell viability.

## INTRODUCTION

Sister chromatid cohesion is essential for faithful chromosome segregation in eukaryotic cells. The cohesin complex is essential not only for genome segregation, but also for the maintenance of genome integrity, regulation of transcription, the determination of genome architecture and DNA damage repair (Haarhuis et al., 2014; Parelho et al., 2008; Peters and Nishiyama, 2012; Sjögren and Nasmyth, 2001; Yan et al., 2013).

The core cohesin complex consists of an annular trimer comprising two SMC proteins, Smc1 and Smc3, and the alpha-kleisin subunit Mcd1/Scc1. Each SMC protein contains an ATPase head, composed of two lobes contributed by their N and C termini, and a central hinge domain, which are separated by ~40 nm through the antiparallel packing of the intervening coiled-coil region. Smc3 and Smc1 heterodimerize through the hinge domains, and their ATPase heads associate with the N- and C-terminal domains of Scc1, respectively. The resulting assemblies are large tripartite rings, which are thought to topologically entrap sister chromatids (Gligoris et al., 2014;

Gruber et al., 2003; Haering et al., 2008; Huis in 't Veld et al., 2014).

Turnover of the complex on DNA remains dynamic until S phase, when stable cohesion is established by the acetylation of Smc3 by the cohesin acetyltransferase Eco1 (Rolef Ben-Shahar et al., 2008; Unal et al., 2008; Zhang et al., 2008). Acetylated cohesin then remains robustly associated with chromosomes until proteolytic cleavage of the Scc1 subunit, by the cysteine protease Separase, at the metaphase-to-anaphase transition releases sister chromatids for segregation into daughter cells (Peters and Nishiyama, 2012; Rowland et al., 2009; Sutani et al., 2009; Tedeschi et al., 2013). Release of intact cohesin from chromatin appears to be mediated through transient disruption of the Smc3-Scc1 interface and allows the complex to participate in dynamic cycles of DNA entrapment and release (Buheitel and Stemann, 2013; Chan et al., 2012; Eichinger et al., 2013). Cohesin release is exquisitely controlled by a series of accessory proteins: Scc3, Pds5, and the dissociation factor Wapl, which have been proposed to collectively modulate the stability of cohesin on chromatin. The association of these proteins with cohesin occurs through Scc1, which serves as a nexus for the recruitment of regulatory factors (Chan et al., 2012; Hara et al., 2014; Roig et al., 2014; Rowland et al., 2009; Sutani et al., 2009). The appropriate regulation of this release activity is a critical determinant of genome architecture in species ranging from yeast to humans (Guacci and Koshland, 2012; Lopez-Serra et al., 2013; Tedeschi et al., 2013; Yan et al., 2013) and is presumably essential to the roles of cohesin that lie outside the establishment of sister chromatid cohesion.

Of the factors that regulate cohesion, Pds5 remains the most enigmatic. Not only does it mediate the release of cohesin from DNA but is also implicated in establishing and maintaining cohesion by the promotion and preservation of Smc3 acetylation (Rolef Ben-Shahar et al., 2008; Carretero et al., 2013; Chan et al., 2013; Hou and Zou, 2005; Losada et al., 2005; Minamino et al., 2015; Rowland et al., 2009; Shintomi and Hirano, 2009; Unal et al., 2008; Vaur et al., 2012; Zhang et al., 2008). Pds5 is essential for cohesion in yeast (Hartman et al., 2000; Panizza et al., 2000), and in mammals cohesin function is disrupted in the absence of Pds5 (Carretero et al., 2013). Mice lacking either Pds5 isoform fail to complete embryonic development, and cells from Pds5B null mice exhibit aneuploidy, and an impaired spindle assembly checkpoint (Carretero et al., 2013).

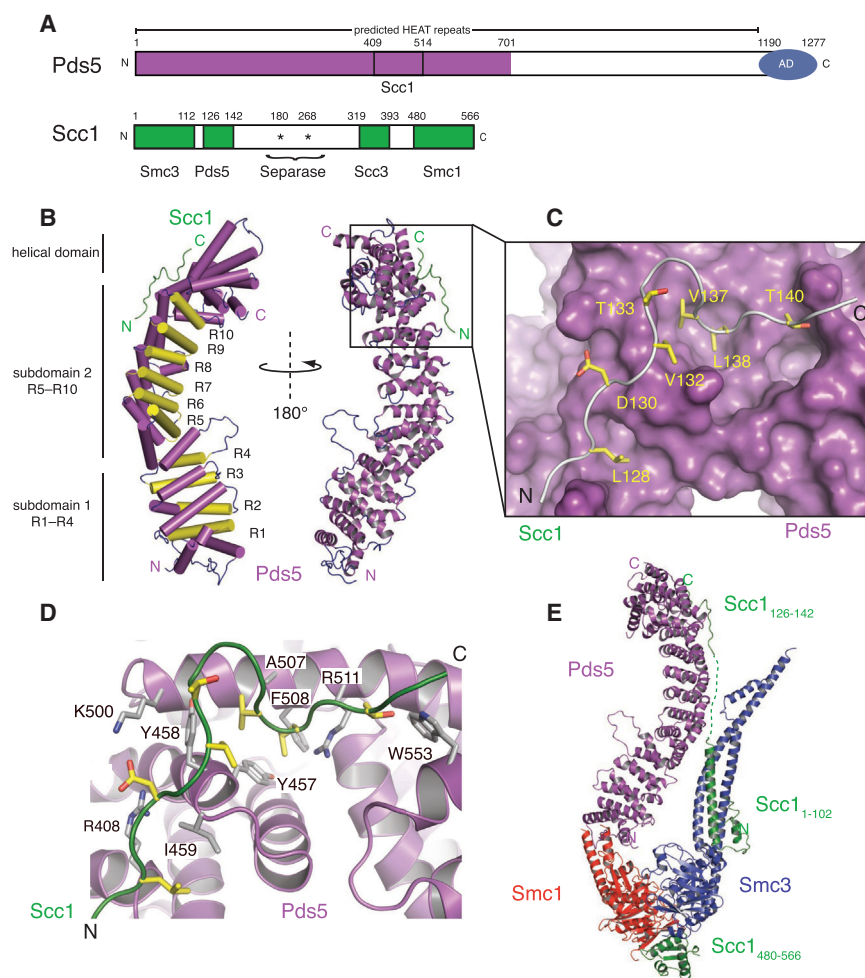


**Figure 1. Structure of the Pds5-Sccl Complex**

(A) Domain architecture of Pds5 and Sccl. Regions involved in complex formation are indicated. (AD; acidic domain).

(B) A ribbon view of Pds5 structure with the HEAT repeats R1–R10 labeled. Pds5 is shown in magenta and Sccl in green. The partner  $\alpha$  helices of the R1–R10 repeats are shown in yellow.

(C) Surface rendered view of the Pds5–Sccl interface. Select Sccl residues are indicated.

(D) View of interactions between Pds5 and Sccl. Select Pds5 residues are labeled. Nitrogen and oxygen atoms are shown in blue and red, respectively. Sccl backbone atoms are colored in green and side-chain carbon atoms in yellow. Pds5 side-chain carbon atoms are in gray.

(E) Hypothetical model of the quaternary Smc1–Smc3–Sccl–Pds5 (colored red, blue, green, and magenta, respectively) complex containing available structural data (PDB codes 1W1W, 4UX3, this study). A flexible linker comprising amino acid residues 103–125 of Sccl (dotted green line) separates Pds5 from the N-terminal fragment (1–102) of Sccl bound to the Smc3Hd.

See also Figure S1.

## RESULTS

Budding yeast Pds5 is a 1,277 amino acid residue protein predicted to contain a HEAT (Huntington, EF3, PP2A, TOR1) repeat domain and a highly charged C-terminal region (Figure 1A). Sccl is a 566-amino-acid residue protein that contains binding sites for the core Smc3 and Smc1 subunits of cohesin in its

conserved N- and C-terminal domains, respectively (Figure 1A). Two Separase cleavage sites are present in the central region of the protein and are flanked by Pds5 and Sccl binding sites. To derive further insight into the function of Pds5 and its interaction with Sccl, we coexpressed these proteins in *Escherichia coli* and used limited proteolysis to identify a Pds5 and Sccl-containing subcomplex. Limited proteolysis yielded stable Pds5 subdomains (Figure S1A) that were cloned and coexpressed with Sccl. Proteolysis of Pds5–Sccl revealed a stable Sccl fragment corresponding to amino acids 116–160 (Figures S1B and S1C). Expression of these proteins in *Escherichia coli* facilitated the purification and crystallization of Pds5T (amino acids 1–701) in isolation, and of Pds5T–Sccl in complex (Figures S1D and S1E). While crystals of Pds5T, in isolation, only diffracted to a minimum Bragg spacing of 5.8 Å, the Pds5T–Sccl complex diffracted to 2.9 Å. Diffraction data collected from selenomethionine-substituted derivatives of the Pds5T–Sccl crystals enabled the determination of initial phases by single wavelength anomalous dispersion (SAD) and the generation of an incomplete model, built into a 3.4-Å resolution map. This model was then employed in phasing the higher resolution data by molecular replacement and enabled us to build a final model containing

Pds5 binds to Sccl in close proximity to the Sccl–Smc3 interface, whose disengagement is thought to be required for dynamic release of DNA from cohesin (Buheitel and Stemmann, 2013; Chan et al., 2012, 2013; Eichinger et al., 2013). Therefore, it is possible that Pds5 exerts its regulatory effect by controlling the opening and closure of this interface. Both activities may require modulation of ATP hydrolysis by the Smc1–Smc3 head domains, the acetylation status of Smc3, and the recruitment of the release factor Wapl (Chan et al., 2013; Shintomi and Hirano, 2009).

Hence, Pds5 is a critical point of convergence for seemingly divergent cohesin functions. In order to clarify molecular basis for the different roles ascribed to Pds5, we have determined the crystal structure of Pds5 in complex with Sccl, from the budding yeast *Saccharomyces cerevisiae*, and investigated the nature of its transactions with cohesin at the Smc3–Sccl interface. Pds5 forms an extended HEAT repeat array that binds a short Sccl fragment through a conserved surface patch. Using a combination of in vitro and in vivo analysis, we demonstrate that this conserved patch is required for recruitment of Pds5 to cohesin and for the maintenance of sister chromatid cohesion.

conserved N- and C-terminal domains, respectively (Figure 1A). Two Separase cleavage sites are present in the central region of the protein and are flanked by Pds5 and Sccl binding sites. To derive further insight into the function of Pds5 and its interaction with Sccl, we coexpressed these proteins in *Escherichia coli* and used limited proteolysis to identify a Pds5 and Sccl-containing subcomplex. Limited proteolysis yielded stable Pds5 subdomains (Figure S1A) that were cloned and coexpressed with Sccl. Proteolysis of Pds5–Sccl revealed a stable Sccl fragment corresponding to amino acids 116–160 (Figures S1B and S1C). Expression of these proteins in *Escherichia coli* facilitated the purification and crystallization of Pds5T (amino acids 1–701) in isolation, and of Pds5T–Sccl in complex (Figures S1D and S1E). While crystals of Pds5T, in isolation, only diffracted to a minimum Bragg spacing of 5.8 Å, the Pds5T–Sccl complex diffracted to 2.9 Å. Diffraction data collected from selenomethionine-substituted derivatives of the Pds5T–Sccl crystals enabled the determination of initial phases by single wavelength anomalous dispersion (SAD) and the generation of an incomplete model, built into a 3.4-Å resolution map. This model was then employed in phasing the higher resolution data by molecular replacement and enabled us to build a final model containing

**Table 1. Data Collection, Phasing, and Refinement Statistics**

	Pds5T-Scc1 Native	Pds5T Native	Pds5T-Scc1 SAD	Pds5T-Scc1 <sup>L128M</sup> SAD
Data collection				
Space group	P2 <sub>1</sub>	I422	P2 <sub>1</sub>	P2 <sub>1</sub>
Cell dimensions				
a, b, c (Å)	147.23, 62.56, 155.94	283.69, 283.69, 172.79	147.30, 62.67, 156.20	148.61, 62.64, 156.89
Wavelength	0.965	0.999	0.965	0.965
Resolution (Å)	50–2.9	50–5.8	50–3.4	50–3.7
R <sub>sym</sub> or R <sub>merge</sub>	4.6 (71.3)	2.3 (51.8)	6.1 (41.2)	19.8 (94.7)
I / σI	9.14 (1.11)	17.19 (1.57)	10.1 (1.8)	8.39 (1.56)
CC (1/2)	99.9 (50.7)	99.9 (61.89)	99.7 (69.6)	0.99 (0.66)
Completeness (%)	96.3 (89.5)	99.3 (98.5)	96.4 (71)	99.2 (93.1)
Redundancy	2.58 (2.55)	7.61 (7.99)	1.99 (1.92)	6.4 (5.1)
Refinement				
Resolution (Å)	50–2.9	50–5.8		50–3.7
No. reflections	59,992	10,082		29,319
R <sub>work</sub> / R <sub>free</sub>	0.265/0.298	0.249/0.311		0.212/0.260
No. atoms	11,116	10,858		11160
Protein	1,371	1,337		1,376
β factors				
Protein	106	424		92
RMSD				
Bond lengths (Å)	0.003	0.003		0.008
Bond angles (°)	0.677	0.611		1.02

Values in parentheses are for highest-resolution shell.

residues 3–610 and 623–697 of Pds5 and residues 126–142 of Scc1 (Table 1). An accompanying report in this issue of *Cell Reports* describes the structure of an additional C-terminal extension of Pds5 in complex with Scc1 (Lee et al., 2016).

### Structure of the Pds5T-Scc1 Complex

As predicted from the amino acid sequence, Pds5T consists of tandem HEAT repeats (designated R1–10), which form a super-helical array. A segment containing an extended loop interrupts the solenoid, such that HEAT repeats R4 and R5 are apposed in a perpendicular fashion. Thus, the HEAT repeats are segregated into two major subdomains: R1–R4 and R5–R10 (Figure 1B). Toward the C terminus, the solenoid is interrupted by a 6 α-helical platform that serves as a scaffold for Scc1 binding. Residues 126–142 of Scc1 form an extended coil that binds along the outer surface of Pds5T, such that its C-terminal end progresses toward the C terminus of Pds5, and terminates along the six α-helical scaffold, perpendicular to the main axis of Pds5 (Figure 1B). Calculation of an electron density map, following molecular replacement in which Scc1 was omitted from the search model, showed obvious positive density for the Scc1 chain (Figure S1F). To validate the register and binding orientation of Scc1, we mutated residue L128 in our Scc1 construct to methionine and produced crystals of selenomethionine-substituted Pds5T-Scc1. An anomalous difference map revealed an additional peak at the expected position and therefore unambiguously confirmed the amino acid register (Figure S1D). The extended conformation of Scc1 depends on its contacts with the surround-

ing Pds5T and so this domain is likely to be unstructured in the absence of its partner. In contrast, Pds5T does not undergo major conformational changes upon binding to Scc1: our 5.8-Å crystal structure of Pds5T in isolation retains an identical conformation to that observed for the Pds5T-Scc1 complex, despite a different crystal packing environment (C<sub>α</sub> root mean square deviation = 0.36 Å<sup>2</sup>; Figure S1E). Engagement of this domain of Scc1 positions Pds5 in close proximity to the Smc1-Smc3 head complex (Figure 1E), as the Smc3 and Pds5 binding regions of Scc1, Scc1<sup>1–102</sup>, and Scc1<sup>126–142</sup>, respectively, are separated by only 24 amino acids. Such close juxtaposition of Pds5 and the Smc1-Smc3 ATPase heads may potentially be of consequence in regulating the closure of the Scc1-Smc3 interface (Buheitel and Stemmann, 2013; Chan et al., 2012; Eichinger et al., 2013; Gligoris et al., 2014; Huis in 't Veld et al., 2014).

Scc1 interacts with Pds5 predominantly through a tridentate projection of hydrophobic residues into three separate hydrophobic pockets. The first hydrophobic pocket containing Pds5<sup>L459</sup> accommodates Scc1<sup>L128</sup> (Figure 1C). Backbone contacts of Pds5<sup>R408</sup> further stabilize this interaction (Figure 1D). Further toward the C terminus, Pds5<sup>R408</sup>, together with Pds5<sup>K500</sup>, participates in electrostatic interactions with Scc1<sup>D130</sup>. The second hydrophobic pocket is the most substantial and robustly anchors Pds5 to Scc1. Additional contacts occur between Scc1<sup>V132</sup> and Pds5<sup>Y458</sup>. Electrostatic interactions between Scc1<sup>T133</sup> and Scc1<sup>E136</sup> curve the peptide and loop the intervening sequence, such that residues Scc1<sup>V137</sup> and Scc1<sup>L138</sup> project deeply into the hydrophobic pocket lined by Pds5<sup>Y457</sup>,

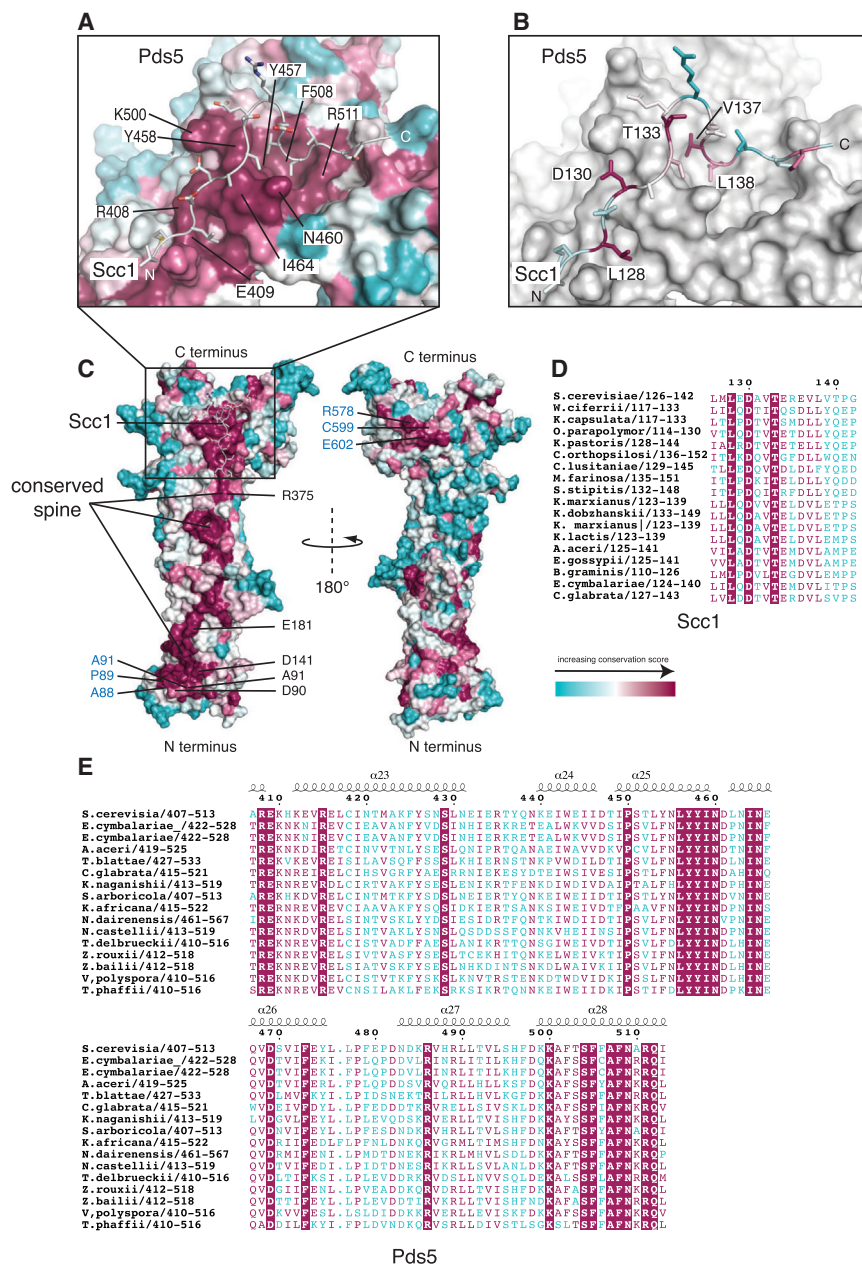


**Figure 2. Sequence Conservation of Pds5 and Scc1**

(A) The region of Pds5 around the Scc1 binding interface is shown and colored according to sequence conservation. Highly conserved residues of Pds5 are indicated.

(B) Sequence conservation of Scc1 is mapped onto the structure and Pds5 is shown in gray. Scc1 residues are shown as sticks and highly conserved Scc1 residues are indicated.

(C) Surface residue conservation of Pds5 (left) including a 180° rotation (right). The conserved Scc1 binding site on Pds5 is part of a larger conserved spine that flows from the N terminus of Pds5. Residues in the conserved spine that were analyzed are indicated in black. Previously published surface-located *eco1-1* suppressor mutants are shown in blue.

(D) Alignment of yeast Scc1 amino acid sequences.

(E) Alignment of yeast Pds5 amino acid sequences.

See also Figure S2.

particular, the chemical properties of residues in the second hydrophobic pocket are highly conserved in divergent eukaryotes, ranging from yeasts to humans (Figures S2A and S2B). Thus, it is likely that the same interface is also relevant for Pds5 and Scc1 function in organisms whose genomes encode orthologous proteins. Furthermore, the conserved Scc1 binding site on Pds5 is part of a larger conserved surface spine that extends toward the N terminus of Pds5 (Figure 2C), which suggests that this region of Pds5 might also be required for other aspects of cohesin function.

### Analysis of the Pds5-Scc1 Interface

To test the relevance of the assembly described in our structure, we performed pull-down assays of Pds5T against a binary complex of the Smc3 head (Smc3Hd) and an N-terminal region of Scc1 encompassing binding sites for both of the larger proteins (NScc1; C-terminal 6 × Histidine tag). The mutation of conserved residues in the Scc1 binding domain of Pds5 abolished (Pds5<sup>R408D</sup>, Pds5<sup>Y457D</sup>, Pds5<sup>Y458A</sup>, Pds5<sup>Y458E</sup>, Pds5<sup>Y457A/Y458A</sup>, Pds5<sup>Y458D/Y458E</sup>, and Pds5<sup>K500E</sup>) or reduced (Pds5<sup>K500E</sup> and Pds5<sup>W533A</sup>) binding to the Smc3Hd-NScc1 complex (Figure 3A). Whereas the Pds5<sup>Y457A</sup> and Pds5<sup>R511A</sup> mutants exhibit essentially wild-type binding. All mutations analyzed are located on the surface of Pds5T and do not interfere with protein stability (Figure S3A). Any impact of these mutations on Scc1 binding is therefore attributable to the perturbation of specific interactions. Consistent with a previous *in vivo* study (Chan et al., 2013), mutation of Scc1<sup>V137G/L138G</sup> abolished binding of Pds5T (Figure 3B)

Pds5<sup>Y458</sup>, and Pds5<sup>Y459</sup>. The third hydrophobic pocket, delimited by Pds5<sup>I515</sup> and abutted by Pds5<sup>W553</sup>, accommodates Scc1<sup>T140</sup> (Figure 1D).

### Conservation of the Pds5-Scc1 Interface

To investigate conserved surface features, which may themselves correspond to conserved functional elements, sequence alignments for Pds5T and Scc1 were compiled and amino acid conservation mapped onto the structure. Amino acid residues of Pds5T buried in the heterodimerization interface are typically conserved, while residues not engaged in the interface are divergent (Figures 2A, 2C, and 2E). Similarly, Scc1 residues facing the interface are also well conserved (Figure 2B). In

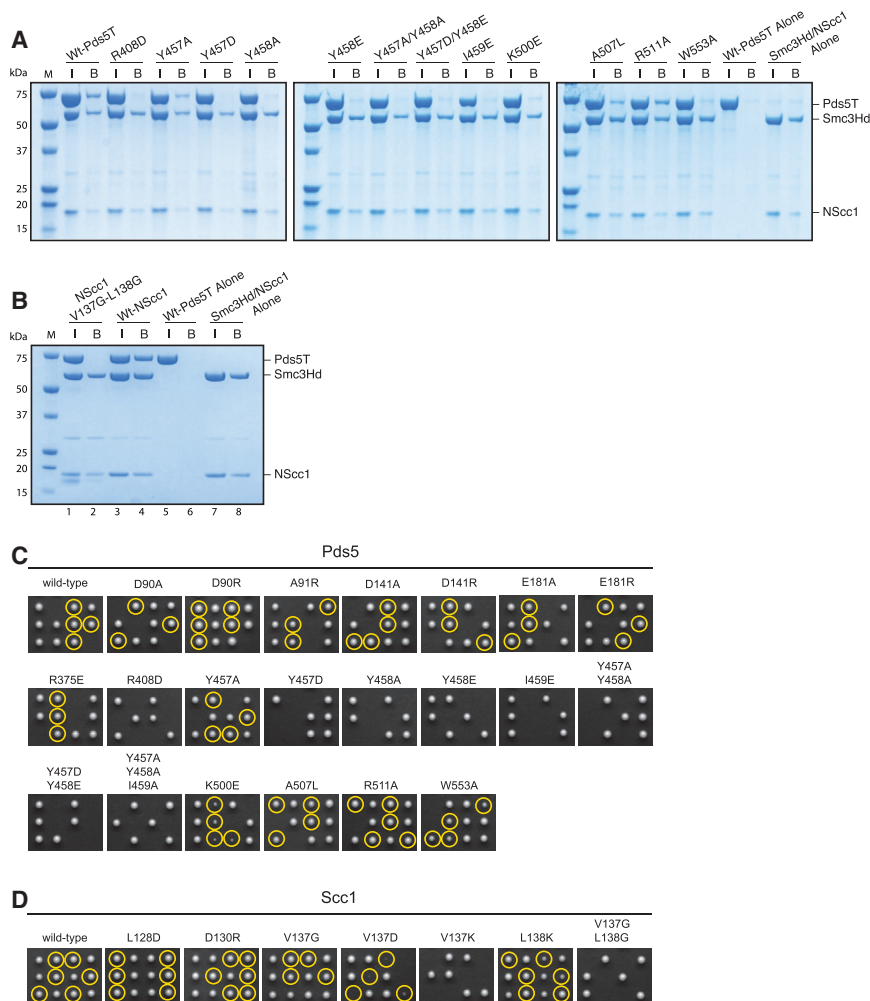


**Figure 3. In Vitro and In Vivo Analysis of Pds5-Scc1 Interaction**

(A) His-tagged Scc3Hd-NScc1 was used to pull down the indicated Pds5T mutants.

(B) The Scc3Hd-NScc1 V137G/L138G mutant (lanes 1, 2) or Scc3Hd-NScc1 wild-type (lanes 3, 4) was used to pull-down wild-type Pds5T. Controls for Pds5T are shown in lanes 5 and 6 and for Scc3Hd-NScc1 in lanes 7 and 8. I, input; B, bound; M, marker.

(C) Diploid PDS5/ $\Delta\Delta\Sigma5$ / yeast cells expressing an ectopic copy of wild-type or mutant Pds5-PK6 were sporulated, tetrad-dissected, and analyzed after 48 hr at 30°C. Three representative tetrads are shown for each mutant. Cells containing the ectopic copy of Pds5 over  $\Delta pds5$  are circled.

(D) Analysis of wild-type or mutant Scc1-HA6 as in (C). Due to genetic linkage between the ectopic copy of Scc1 integrated at the TRP1 locus and the endogenous SCC1 locus, only cells that integrated the ectopic copy of Scc1 on the  $\Delta scc1$  chromosome were analyzed.

See also Figure S3.

As anticipated, mutations in Scc1 that preclude Pds5 binding abolished ( $Scc1^{V137K}$  and  $Scc1^{V137G/L138G}$ ) or reduced ( $Scc1^{V137D}$  and  $Scc1^{L138K}$ ) cell growth (Figure 3D). In contrast, neither the single  $Scc1^{V137G}$  mutation nor the individual mutation of  $Scc1^{L128D}$  and  $Scc1^{D130R}$  had any observable impact on cell growth. As all mutant proteins were expressed at levels equivalent to their wild-type counterparts, these results are specifically attributable to the loss of critical Pds5 and Scc1 functionality (Figures S3C and S3D). We conclude that,

in vitro, confirming the integrity of this hydrophobic interaction is pivotal to the association of Pds5 and Scc1.

Next, we investigated whether the newly revealed Pds5-Scc1 interface is essential for cohesin function in vivo by testing whether mutation of the Pds5-Scc1 interaction impacts cell viability. Mutations in Pds5 that disrupted binding of Pds5T to Scc3Hd-NScc1, in the pull-down assay ( $Pds5^{R408D}$ ,  $Pds5^{Y457D}$ ,  $Pds5^{Y458A}$ ,  $Pds5^{Y458E}$ ,  $Pds5^{Y458A/Y458A}$ ,  $Pds5^{Y458D/Y458E}$ ,  $Pds5^{I459E}$ ,  $Pds5^{Y458A/Y458A/I495A}$ ,  $Pds5^{Y458A/Y458A/I495A}$ ) failed to complement deletion of the essential *PDS5* gene (Figure 3C). Mutations that reduced binding of Pds5T to Scc3Hd-NScc1, ( $Pds5^{K500E}$  and  $Pds5^{W553A}$ ) confer impairment in cell growth proportionate to the weakening of binding strength observed in vitro, and mutations that had no effect on the interaction of Pds5T with Scc3Hd-Scc1 in vitro did not appreciably alter cell growth ( $Pds5^{Y457A}$ ,  $Pds5^{A507L}$ ,  $Pds5^{R511A}$ ). A lower resolution Pds5T-Scc1 structure features an extension of Scc1 not present in the electron density of the original crystal, which reveals that  $Pds5^{W553}$  also interacts with  $Scc1^{L143}$ , and may provide further explanation for the severity of phenotypes observed for this mutant (Figure S3B).

as diminished binding affinity observed in vitro directly correlates with reduced cell growth, the Pds5-Scc1 interface identified in our crystal structure is a necessary requirement for cohesin function in vivo.

To assess the functional importance of the conserved surface spine (Figure 2C), we mutated a series of residues along its length ( $Pds5^{D90A}$  or  $R$ ,  $Pds5^{A91R}$ ,  $Pds5^{D141R}$ ,  $Pds5^{E181R}$  and  $Pds5^{R375E}$  as shown in Figure 2C). However, individual mutations within this spine have no apparent effect on cell growth (Figure 3C). Prior studies identified a series of mutations in the N-terminal region of Pds5 that suppress inactivation of the temperature sensitive *eco1-1* allele in yeast (Rowland et al., 2009; Sutani et al., 2009). Of the surface-exposed suppressor mutations, the majority ( $Pds5^{A88D}$  or  $P$ ,  $Pds5^{P89S}$  or  $Q$  or  $L$  and  $Pds5^{A91T}$ ) cluster around the highly conserved  $Pds5^{D90}$ , suggesting that the surrounding negatively charged patch might function prominently in the control of Pds5-mediated cohesin release activity (Figures S3E and S3F). The observation that a large fraction of *eco1-1* suppressor mutants are situated within or close to the conserved surface of Pds5 suggests that these elements of Pds5 might somehow function in regulating cohesin release.

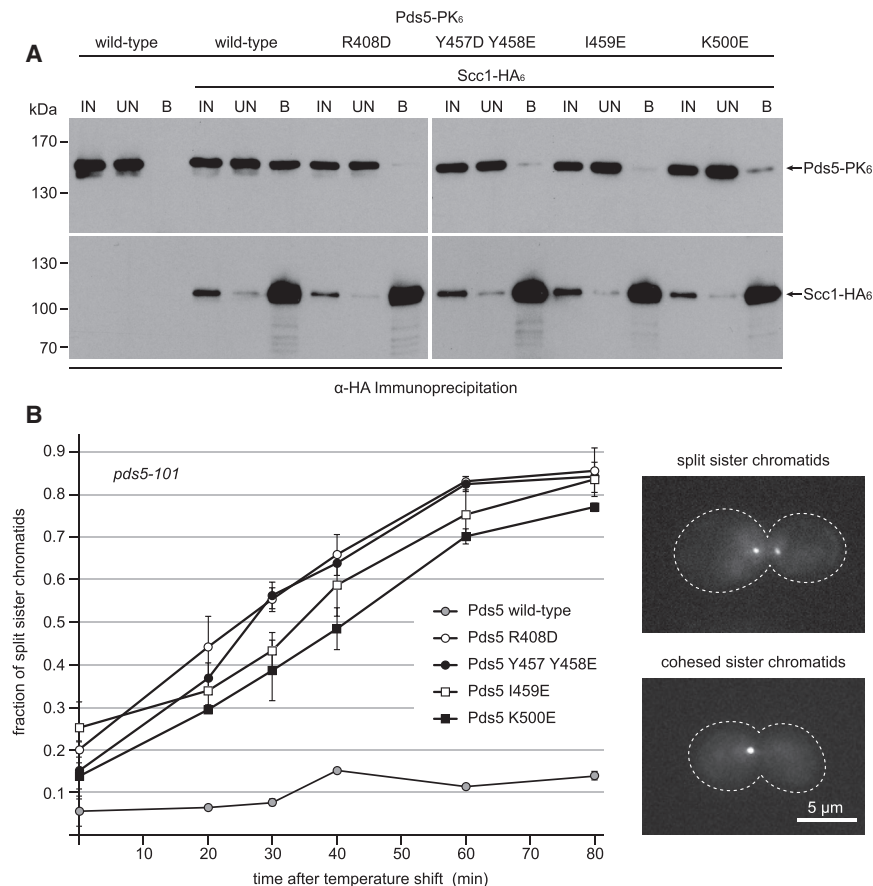


**Figure 4. Cohesin Binding Mutants of Pds5 Fail to Maintain Sister Chromatid Cohesion**

(A) Co-immunoprecipitation of Scc1-HA<sub>6</sub> from whole-cell extracts of asynchronous yeast cultures expressing ectopic copies of the indicated Pds5-PK<sub>6</sub> variants (wild-type and mutants) IN, input; UN, unbound; and B, bound; 17 × relative to input for Pds5, 42.5 × for Scc1) fractions.

(B) Sister chromatid cohesion was assayed in cells expressing wild-type or mutant Pds5-PK<sub>6</sub> in a *pds5-101* temperature-sensitive background. Cells were arrested in metaphase by Cdc20 depletion, shifted to the restrictive temperature, and released. The fraction of cells with split sister chromatids at time points after shifting to the restrictive temperature was determined for >100 cells per time point and strain. Mean values (±max/min) of two independent repeats per mutant are plotted. See also Figure S4.

tored the separation of fluorescently labeled sister chromatid loci (Michaelis et al., 1997; Panizza et al., 2000). Whereas cells expressing ectopic copies of wild-type Pds5 were competent to maintain sister chromatid cohesion, cells that expressed any of the mutant Pds5 versions rapidly lost cohesion (Figure 4B). Loss of cohesion was slightly less severe for the Pds5<sup>K500E</sup> mutant, which maintains residual viability and binding to Scc1. Collectively, these data demonstrate that the

### Pds5-Scc1 Interface Mutants Are Defective in Maintenance of Sister Chromatid Cohesion

To confirm that the identified Pds5-Scc1 interaction site is essential for recruitment of Pds5 to cohesin in vivo, we first investigated whether mutations in Pds5 that disrupt the interaction with Scc1 in vitro also do so within the context of the native yeast cohesin complex. Co-immunoprecipitation of Pds5 mutants that affect the salt bridge (Pds5<sup>R408D</sup>, Pds5<sup>K500E</sup>) and hydrophobic interactions (Pds5<sup>Y457D/Y458E</sup>, Pds5<sup>I459E</sup>) with HA-tagged Scc1 produced phenotypes concordant with the in vitro pull-down assays (Figure 4A). Whereas Pds5<sup>R408D</sup>, Pds5<sup>Y457D/Y458E</sup>, and Pds5<sup>I459E</sup> abolished the association of Pds5 with cohesin in this assay, Pds5<sup>K500E</sup> retained modest binding. As disruption of critical residues in the Pds5-Scc1 interface is sufficient to abolish Pds5 recruitment to yeast holocomplexes in vivo, and to the Smc3Hd-NScc1 complex in vitro, we conclude that robust interactions between Pds5 and cohesin appear to be exclusively mediated through the Pds5-Scc1 interface described in our structure.

To directly investigate the influence of Pds5 interface mutations on sister chromatid cohesion, we expressed wild-type or interface mutants Pds5 from an ectopic copy in a *pds5-101* temperature-sensitive strain (Figure S4A) (Panizza et al., 2000). We arrested cells in metaphase by depletion of Cdc20 (Figure S4B), inactivated *pds5-101* by shifting cells to the restrictive temperature and moni-

inviability of Pds5-Scc1 interface mutants arises from the inability of the mutant Pds5 proteins to interact with cohesin, and their consequent failure to functionally contribute to sister chromatid cohesion.

### A Structural Model of the Pds5-Smc3-Scc1 Complex

Multiple roles have been ascribed to Pds5 in the regulation of the cohesin complex. In addition to promoting cohesion, Pds5 also participates in the removal of cohesin from chromatin, apparently by interacting with the dissociation factor Wapl (Chan et al., 2012; Kueng et al., 2006; Losada et al., 2005; Nishiyama et al., 2010; Rowland et al., 2009; Shintomi and Hirano, 2009; Sutani et al., 2009). Acetylation of Smc3<sup>K112/K113</sup> by Eco1 is a key determinant of sister chromatid cohesion and is thought to interfere with this cohesin release function of Pds5 (Chan et al., 2012; Rowland et al., 2009; Sutani et al., 2009). Our structure shows that Pds5 binds in close proximity to the Smc3Hd (Figure 1E); therefore, it is possible that Pds5 might somehow monitor the acetylation status of cohesin and so regulate opening or closure of the ring (Chan et al., 2012).

To investigate this possibility, we isolated a ternary complex comprised of Pds5T-Smc3Hd-NScc1 (Figure 5A) and sought to characterize this assembly in solution by small angle X-ray scattering (SAXS; Figures 5B and 5C). To reduce confounding inter-particle interference and aggregation effects, we collected

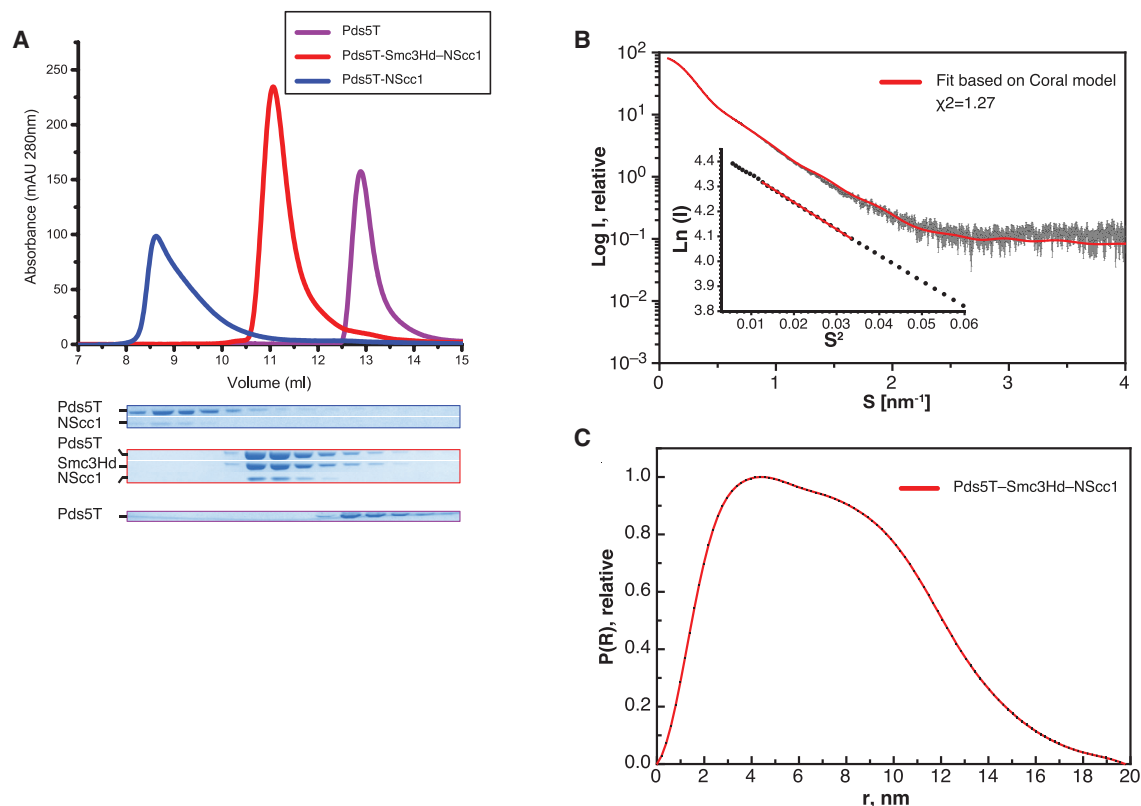


**Figure 5. SAXS Analysis of the Pds5T-Smc3Hd-NScc1 Complex**

(A) Size-exclusion chromatography profiles for Pds5T, Pds5T-NScc1, and the Pds5T-Smc3Hd-NScc1 complex. Fractions from each run were analyzed by SDS-PAGE. Coomassie-stained bands corresponding to each protein are indicated. Gels were cropped to show the relevant sections.

(B) Experimental SAXS profile (log intensities calculated as a function of momentum transfer) for the Pds5T-Smc3Hd-NScc1 complex is shown (black) and the fitted curve (red) obtained using CORAL. The Guinier region is inset. Points 10–25 were used for analysis and showed an  $s^*R_g = 1.06$  (values <1.3 indicate good quality data).

(C) Distance distribution function.

See also Figure S5.

scattering data using an in-line size exclusion chromatography system (Pernot et al., 2013). The scattering profile showed no aggregation and a linear Guinier range, indicative of well-behaved, monodisperse sample (Figure 5B and inset). From these data, we obtained a radius of gyration ( $R_g$ ) of  $56 \pm 0.5 \text{ \AA}$ . The distance distribution function  $p(r)$  displayed a skewed shape characteristic of elongated, multi-domain particles, with a maximum diameter ( $D_{\max}$ ) of  $198 \pm 10 \text{ \AA}$  (Figure 5C). As structural models for almost the entire complex except the Scc1<sup>103–125</sup> linker were available, we evaluated the scattering curves by rigid body modeling using the atomic models for Smc3Hd-Scc1<sup>1–102</sup> and Pds5T-Scc1<sup>126–142</sup> and modeled the missing amino acid residues, including the Scc1<sup>103–125</sup> linker, using Coral (Petoukhov et al., 2012). While resultant models of the ternary complex conform very well ( $\chi^2 = 1.27$ ) to the SAXS data (a representative fit is depicted in Figure S5A), we found that the ternary assembly does not adopt a single unique conformation in solution. In agreement with biochemical and cell biological analyses demonstrating that Pds5 is recruited to cohesin exclusively through Scc1, these data reveal that the conserved surface of Pds5T does not stably engage the Smc3Hd domain. However, we

cannot exclude that other missing parts of the proteins engage in direct interactions, nor the possibility that the interaction between Pds5 and Smc3 might be more dynamic than can be appreciated through such experimental approaches.

## DISCUSSION

Pds5 is a highly conserved regulator of cohesin function, with diverse roles in sister chromatid cohesion. Paradoxically, Pds5 not only participates in the establishment and maintenance of cohesion, but also collaborates with Wapl and Scc3 to promote the release of cohesin from chromatin (Hartman et al., 2000; Panizza et al., 2000; Vaur et al., 2012). To advance our understanding of the multiple functions associated with Pds5, we have determined the structure of Pds5 in complex with a fragment of Scc1. Our structure comprises a large N-terminal fragment of Pds5, including regions that have been previously shown to be critical for Pds5 release function (Rowland et al., 2009; Sutani et al., 2009), and a segment of Scc1 that is required for the interaction of Pds5 with cohesin (Chan et al., 2013). Through a series of biochemical and in vivo experiments, we found that the

disruption of key features of the Pds5–Scc1 interface revealed by the structure abolishes Pds5 recruitment to cohesin. We further establish that the minimal Pds5–Scc1 interface is necessary and sufficient for recruitment of Pds5 to the cohesin complex, and is critical for sister chromatid cohesion.

### A Conserved Interaction Surface Mediates Pds5 Recruitment to Cohesin

Whereas the requirement for Pds5 in sister chromatid cohesion is well established, it has remained controversial in which stages of the cohesin cycle it participates. Early experiments pointed toward a model in which Pds5 is uniquely required for maintenance of cohesion, but not its establishment (Hartman et al., 2000; Stead et al., 2003). Initial observations suggested that the interaction of Pds5 with human cohesin is salt sensitive; thus, it was proposed that Pds5 might therefore constitute a transiently bound regulatory factor, rather than a bona fide cohesin subunit (Gandhi et al., 2006; Kueng et al., 2006; Losada et al., 2005; Panizza et al., 2000; Sumara et al., 2000). However, it was recently reported that Pds5 both promotes Smc3 acetylation and antagonizes its deacetylation, and thereby contributes not only to maintenance but also the establishment of cohesion (Carretero et al., 2013; Chan et al., 2013; Vaur et al., 2012).

Furthermore, as the deletion of either Pds5 isoform in mice is lethal, it is evident that Pds5 function is also essential in vertebrates (Carretero et al., 2013). Therefore, there is an increasing body of evidence to suggest that, from yeast to humans, Pds5, like the other cohesin components, is essential to both establishment and maintenance of cohesion (Carretero et al., 2013; Chan et al., 2013; Hartman et al., 2000; Losada et al., 2005; Panizza et al., 2000; Vaur et al., 2012).

We observed a strong correlation between the strength of the Pds5–Scc1 interaction, cell viability, and the maintenance of sister chromatid cohesion, which suggests that the persistent recruitment of Pds5 is integral to cohesin function. In particular, the failure of the partial binding mutant, Pds5<sup>K500E</sup>, to support cohesion at the restrictive temperature for *pds5-101* suggests that enduring cohesion requires correspondingly robust Pds5–cohesin assemblies. However, further studies will be required to investigate if Pds5 is continuously and stoichiometrically bound to the cohesin complex throughout the cell cycle. The Pds5–Scc1 interface is highly conserved across diverse eukaryotes. We would suggest therefore that the mechanism of recruitment we describe here is a general and necessary feature of cohesin function in all organisms containing Pds5. Differences in phenotypes observed upon disruption of Pds5 in *Schizosaccharomyces pombe* might reflect divergent modes of cohesion establishment and maintenance in this organism (Tanaka et al., 2001; Vaur et al., 2012).

### Role of Pds5 in Regulating the Smc3–Scc1 Interface

Not only does Pds5 contribute to the establishment and maintenance of cohesion, conversely, Pds5 also controls the release of cohesin from chromatin in collaboration with Wapl and Scc3 (Chan et al., 2013; Gandhi et al., 2006; Rowland et al., 2009; Shintomi and Hirano, 2009; Sutani et al., 2009). As Pds5 binds in close proximity to the Smc3Hd, one might envision that it could control Smc3 acetylation, and thus the stable closure of

the cohesin ring, by binding directly to the region surrounding Smc3<sup>K112/113</sup>.

Calculation of the electrostatic surface potential shows that the conserved N-terminal region of Pds5 is highly negatively charged (Figure S5B). It is therefore conceivable that this region of Pds5 monitors the lysine acetylation status of Smc3Hd. However, we found no evidence that Pds5 binds stably to the Smc3Hd while also bound to Scc1, as ablation of key residues on Pds5 and Scc1 alone is sufficient to preclude assembly of this ternary complex in vitro and in vivo. The SAXS data further suggest that, at least in the absence of acetylation, Pds5 and the Smc3Hd do not adopt a single preferred conformation in solution.

Several studies have shown that Wapl directly interacts with Pds5 to execute the removal of cohesin from chromatin (Rowland et al., 2009; Shintomi and Hirano, 2009; Sutani et al., 2009). Such an interaction was proposed to occur through the conserved N-terminal domain of Pds5, as suppressor mutations in this region abolish co-localization of Wapl and cohesin in vivo (Chan et al., 2012). Hence, one possibility might be that the N terminus of Pds5 positions Wapl in the vicinity of the Smc3–Scc1 interface. However, we were not able to isolate a stable complex between Wapl and Pds5T or full-length Pds5 using biochemically well-defined protein preparations (Figures S5C and S5D), nor could we detect persistent interactions between Wapl and the ternary Pds5T–Smc3Hd–NScc1 complex (Figure S5E). However, we cannot exclude that Pds5 interacts directly with Wapl when part of the cohesin holocomplex.

A preponderance of evidence exists to suggest that the binding of Wapl to cohesin is likely a highly co-operative event, and so the finding that Pds5 does not directly interact with Wapl in our in vitro assay is not altogether irreconcilable with the notion that they might still interact functionally in vivo (Gandhi et al., 2006; Hara et al., 2014; Huis in 't Veld et al., 2014; Kueng et al., 2006; Ouyang et al., 2013; Shintomi and Hirano, 2009). Since fusion of the Smc3–Scc1 interface antagonizes cohesin release, the possibility remains that the accessibility of NScc1 and its engagement by Wapl is of functional relevance and might be a key determinant of whether cohesin is released from DNA (Buheitel and Stemmann, 2013; Chan et al., 2012; Eichinger et al., 2013; Gligoris et al., 2014).

The structure reveals that Pds5 contains a highly conserved and almost continuous surface spine that extends from the N terminus of Pds5 toward the Scc1 binding region. The positions of conserved surface residues along this spine correlate with those of *eco1-1* suppressor mutants and are particularly enriched in a highly negative patch located in the Pds5 N terminus (Figure S5B) (Chan et al., 2012; Sutani et al., 2009). Hence, it is possible that this patch on Pds5 might contribute to the efficient disengagement of cohesin from chromatin, in cooperation with other release factors such as Wapl. As deletion of Wapl alone does not lead to inviability in budding yeast, this may present an explanation as to why the alteration of this conserved spine does not impair cell growth (Chan et al., 2013; Lopez-Serra et al., 2013; Rowland et al., 2009; Sutani et al., 2009).

In metazoans, Pds5 is universally conserved and may act, through the conserved spine, as a crucial and indispensable regulator of the dynamic cellular population of cohesin and its

higher-order transactions with chromatin (Haarhuis et al., 2013, 2014; Shintomi and Hirano, 2009; Yan et al., 2013). As Pds5 alone is not able to disengage Smc3 and Scc1, it is likely that this function, appropriately, is restricted to a very specific context in the cell and may depend on additional factors and biochemical events, such as Wapl and ATP hydrolysis (Murayama and Uhlmann, 2015; Shintomi and Hirano, 2009). Indeed, it could be that the function of Sororin, a Pds5-binding metazoan cohesion factor, might confer an enhancement in cohesion by restricting access to this “releasing” patch on Pds5, until it is required to participate in cohesin release during prophase; however, this possibility remains to be explored (Nishiyama et al., 2010, 2013).

In agreement with previously published data showing that Pds5 colocalizes and turns over with core cohesin components and participates in the key functional steps of cohesion, we found that the specific abrogation of Pds5 recruitment to cohesin results in a stark failure to maintain sister chromatid cohesion (Carretero et al., 2013; Chan et al., 2012, 2013; Hartman et al., 2000; Losada et al., 2005; Panizza et al., 2000; Vaur et al., 2012). Furthermore, the Pds5-Scc1 structure reveals an extended surface spine whose conserved residues correlate with those previously determined to be important in control of cohesin release (Chan et al., 2012; Rowland et al., 2009; Sutani et al., 2009).

Thus, our work demonstrates that Pds5 is physically positioned to act as a critical bifunctional regulator of the closure of the ring at the Smc3-Scc1 interface, and therefore of the stable establishment and maintenance of cohesion and, conversely, the dynamic release of cohesin.

Future studies will be required to address at a mechanistic level how Pds5 might coordinate the transition between the opening and stable closure of the Smc3-Scc1 interface, and how these mechanisms might, in turn, facilitate different functions of the cohesin complex.

## EXPERIMENTAL PROCEDURES

### Crystallization and Data Collection

Initial screening of Pds5T and Pds5T-Scc1 was performed by the EMBL Grenoble HTX laboratory. Pds5T was first crystallized in 0.1 M MES (pH 6) and 1.6 M ammonium sulfate. Crystals from which data were collected grew in 1.5 M lithium sulfate, 0.1 M MES (pH 6.5), grown at 4°C, using manually set hanging drops and vapor diffusion and were cryoprotected in a solution containing 2 M lithium sulfate and 0.1 M MES (pH 6.5). The Pds5T-Scc1 complex first crystallized in 0.1 M MES (pH 6.5), 15% MPD. Pds5T-Scc1 crystals were manually refined and were directly flash-frozen in liquid nitrogen without additional cryoprotectant prior to data collection. Diffraction data for native and selenomethionine-derivatized Pds5T-Scc1 were collected at 100°K at an X-ray wavelength of 0.966 Å at beamline ID30A-1/MASSIF-1 of the European Synchrotron Radiation Facility, with a Pilatus 6M-F detector (Svensson et al., 2015). Diffraction data for Pds5T were collected separately at beamline ID23-2 of the ESRF, at 100°K at an X-ray wavelength of 0.999 Å. All data processing was performed with XDS (Kabsch, 2010) and imported into CCP4 format using AIMLESS (Winn et al., 2011).

### Structure Determination, Refinement, and Analysis

The structure of the Pds5-Scc1 complex was determined by single-wavelength anomalous dispersion (SAD) in space group P2<sub>1</sub> at a resolution of 3.4 Å from a selenomethionine-labeled crystal. Heavy atom parameter refinement and SAD phase calculations were performed with SHARP using anom-

alous signal from 12 selenomethionine sites. The electron density map was improved by the application of solvent flattening using PARROT. A final model of the Pds5-Scc1 complex was produced by iterative rounds of manual model building and refinement, using Coot and PHENIX (Adams et al., 2010; Emsley and Cowtan, 2004). The final Pds5-Scc1 complex model containing residues 3–697 of Pds5 and 126–142 of Scc1 was refined to a resolution of 2.9 Å with an R<sub>work</sub> and an R<sub>free</sub> of 26.5% and 29.8%, respectively. No electron density was observed for residues 610–623 in Pds5. The register of Scc1 was verified by an anomalous difference map, generated from diffraction data collected from a selenomethionine-labeled Scc1<sup>L128M</sup> mutant. Analysis of the refined structure in MolProbity showed that there no residues in disallowed regions of the Ramachandran plot. The MolProbity all atom clash score was 5.77, placing the structure in the 100<sup>th</sup> (best) percentile of structures (n = 97) refined at comparable resolution (Chen et al., 2010). The structure of apo Pds5T was determined by molecular replacement with Pds5T 3–697, at a resolution of 5.8 Å in space group I422. The initial model was used as both a starting and reference model for subsequent Deformable Elastic Network (DEN) refinement using CNS over a grid-enabled web-server hosted by SBGrid (O'Donovan et al., 2012; Schröder et al., 2010). The refinement protocol was similar to that previously published (Brunger et al., 2012) with the following non-default setting: only a single overall anisotropic B-factor refinement was carried out per chain. DEN restraints and non-crystallographic symmetry (NCS) restraints were maintained throughout the refinement procedure. Seven different temperatures (from 0 to 3,000 K) were tested in the slow-cooling simulated annealing scheme. Of the resulting models, the one with the lowest R<sub>free</sub> value (31.1%) was selected for subsequent analysis. The final structures were visualized in PyMOL (Schrodinger, 2010). All models have no Ramachandran outliers, good stereochemical parameters, and low crystallographic R<sub>work</sub>/R<sub>free</sub>, indicating a good agreement with the diffraction data (Table 1).

## ACCESSION NUMBERS

Atomic coordinates and structure factors of the reported crystal structures have been deposited in the Protein Data Bank under ID codes PDB: 5frp, 5frr, and 5frs.

## SUPPLEMENTAL INFORMATION

Supplemental Information includes Supplemental Experimental Procedures, five figures, and one table and can be found with this article online at <http://dx.doi.org/10.1016/j.celrep.2016.01.078>.

## AUTHOR CONTRIBUTIONS

K.W.M. conceived the project. K.W.M. identified and crystallized Pds5T and Pds5T-Scc1. Biochemical assays were designed and performed by K.W.M. Y.L. performed the Pds5-Wapl pull-down and contributed reagents. Crystal structures were determined by D.P. and K.W.M. M.K. and C.H.H. performed yeast-complementation analyses. M.K. and J.M. performed co-immunoprecipitation experiments and cohesion assays with advice from C.H.H. D.P. advised and assisted on all aspects of the project. K.W.M., C.H.H., and D.P. wrote the manuscript. All authors discussed the results and commented on the manuscript.

## ACKNOWLEDGMENTS

We thank the staff of ESRF and EMBL-Grenoble for assistance and support in using beamlines ID29, ID23-2, BM29, and MASSIF. We thank J. Kirkpatrick and L. Signor for assistance with mass spectrometry. We thank Siyi Zhang for support during early stages of the project.

Received: November 20, 2015

Revised: December 28, 2015

Accepted: January 28, 2016

Published: February 25, 2016

## REFERENCES

- Adams, P.D., Afonine, P.V., Bunkóczi, G., Chen, V.B., Davis, I.W., Echols, N., Headd, J.J., Hung, L.W., Kapral, G.J., Grosse-Kunstleve, R.W., et al. (2010). PHENIX: a comprehensive Python-based system for macromolecular structure solution. *Acta Crystallogr. D Biol. Crystallogr.* **66**, 213–221.
- Brunger, A.T., Adams, P.D., Fromme, P., Fromme, R., Levitt, M., and Schröder, G.F. (2012). Improving the accuracy of macromolecular structure refinement at 7 Å resolution. *Structure* **20**, 957–966.
- Buheitel, J., and Stemmann, O. (2013). Prophase pathway-dependent removal of cohesin from human chromosomes requires opening of the Smc3-Scc1 gate. *EMBO J.* **32**, 666–676.
- Carretero, M., Ruiz-Torres, M., Rodríguez-Corsino, M., Barthelemy, I., and Losada, A. (2013). Pds5B is required for cohesin establishment and Aurora B accumulation at centromeres. *EMBO J.* **32**, 2938–2949.
- Chan, K.L., Roig, M.B., Hu, B., Beckouët, F., Metson, J., and Nasmyth, K. (2012). Cohesin's DNA exit gate is distinct from its entrance gate and is regulated by acetylation. *Cell* **150**, 961–974.
- Chan, K.L., Gligoris, T., Upcher, W., Kato, Y., Shirahige, K., Nasmyth, K., and Beckouët, F. (2013). Pds5 promotes and protects cohesin acetylation. *Proc. Natl. Acad. Sci. USA* **110**, 13020–13025.
- Chen, V.B., Arendall, W.B., 3rd, Headd, J.J., Keedy, D.A., Immormino, R.M., Kapral, G.J., Murray, L.W., Richardson, J.S., and Richardson, D.C. (2010). MolProbity: all-atom structure validation for macromolecular crystallography. *Acta Crystallogr. D Biol. Crystallogr.* **66**, 12–21.
- Eichinger, C.S., Kurze, A., Oliveira, R.A., and Nasmyth, K. (2013). Disengaging the Smc3/kleisin interface releases cohesin from *Drosophila* chromosomes during interphase and mitosis. *EMBO J.* **32**, 656–665.
- Emsley, P., and Cowtan, K. (2004). Coot: model-building tools for molecular graphics. *Acta Crystallogr. D Biol. Crystallogr.* **60**, 2126–2132.
- Gandhi, R., Gillespie, P.J., and Hirano, T. (2006). Human Wapl is a cohesin-binding protein that promotes sister-chromatid resolution in mitotic prophase. *Curr. Biol.* **16**, 2406–2417.
- Gligoris, T.G., Scheinost, J.C., Bürmann, F., Petela, N., Chan, K.L., Uluocak, P., Beckouët, F., Gruber, S., Nasmyth, K., and Löwe, J. (2014). Closing the cohesin ring: structure and function of its Smc3-kleisin interface. *Science* **346**, 963–967.
- Gruber, S., Haering, C.H., and Nasmyth, K. (2003). Chromosomal cohesin forms a ring. *Cell* **112**, 765–777.
- Guacci, V., and Koshland, D. (2012). Cohesin-independent segregation of sister chromatids in budding yeast. *Mol. Biol. Cell* **23**, 729–739.
- Haarhuis, J.H., Elbatsh, A.M., van den Broek, B., Camps, D., Erkan, H., Jalink, K., Medema, R.H., and Rowland, B.D. (2013). WAPL-mediated removal of cohesin protects against segregation errors and aneuploidy. *Curr. Biol.* **23**, 2071–2077.
- Haarhuis, J.H., Elbatsh, A.M., and Rowland, B.D. (2014). Cohesin and its regulation: on the logic of X-shaped chromosomes. *Dev. Cell* **31**, 7–18.
- Haering, C.H., Farcas, A.M., Arumugam, P., Metson, J., and Nasmyth, K. (2008). The cohesin ring concatenates sister DNA molecules. *Nature* **454**, 297–301.
- Hara, K., Zheng, G., Qu, Q., Liu, H., Ouyang, Z., Chen, Z., Tomchick, D.R., and Yu, H. (2014). Structure of cohesin subcomplex pinpoints direct shugoshin-Wapl antagonism in centromeric cohesion. *Nat. Struct. Mol. Biol.* **21**, 864–870.
- Hartman, T., Stead, K., Koshland, D., and Guacci, V. (2000). Pds5p is an essential chromosomal protein required for both sister chromatid cohesion and condensation in *Saccharomyces cerevisiae*. *J. Cell Biol.* **151**, 613–626.
- Hou, F., and Zou, H. (2005). Two human orthologues of Eco1/Ctf7 acetyltransferases are both required for proper sister-chromatid cohesion. *Mol. Biol. Cell* **16**, 3908–3918.
- Huis in 't Veld, P.J., Herzog, F., Ladurner, R., Davidson, I.F., Piric, S., Kreidl, E., Bhaskara, V., Aebersold, R., and Peters, J.M. (2014). Characterization of a DNA exit gate in the human cohesin ring. *Science* **346**, 968–972.
- Kabsch, W. (2010). Xds. *Acta Crystallogr. D Biol. Crystallogr.* **66**, 125–132.
- Kueng, S., Hegemann, B., Peters, B.H., Lipp, J.J., Schleiffer, A., Mechtler, K., and Peters, J.M. (2006). Wapl controls the dynamic association of cohesin with chromatin. *Cell* **127**, 955–967.
- Lee, B.-G., Roig, M.B., Jansma, M., Petela, N., Metson, J., Nasmyth, K., and Löwe, J. (2016). Crystal structure of the cohesin gatekeeper Pds5 and in complex with kleisin Scc. *Cell Rep.* **14**, this issue, 2108–2115.
- Lopez-Serra, L., Lengronne, A., Borges, V., Kelly, G., and Uhlmann, F. (2013). Budding yeast Wapl controls sister chromatid cohesion maintenance and chromosome condensation. *Curr. Biol.* **23**, 64–69.
- Losada, A., Yokochi, T., and Hirano, T. (2005). Functional contribution of Pds5 to cohesin-mediated cohesion in human cells and *Xenopus* egg extracts. *J. Cell Sci.* **118**, 2133–2141.
- Michaelis, C., Ciosk, R., and Nasmyth, K. (1997). Cohesins: chromosomal proteins that prevent premature separation of sister chromatids. *Cell* **91**, 35–45.
- Minamino, M., Ishibashi, M., Nakato, R., Akiyama, K., Tanaka, H., Kato, Y., Negishi, L., Hirota, T., Sutani, T., Bando, M., and Shirahige, K. (2015). Esco1 Acetylates Cohesin via a Mechanism Different from That of Esco2. *Curr. Biol.* **25**, 1694–1706.
- Murayama, Y., and Uhlmann, F. (2015). DNA Entry into and Exit out of the Cohesin Ring by an Interlocking Gate Mechanism. *Cell* **163**, 1628–1640.
- Nishiyama, T., Ladurner, R., Schmitz, J., Kreidl, E., Schleiffer, A., Bhaskara, V., Bando, M., Shirahige, K., Hyman, A.A., Mechtler, K., and Peters, J.M. (2010). Sororin mediates sister chromatid cohesion by antagonizing Wapl. *Cell* **143**, 737–749.
- Nishiyama, T., Sykora, M.M., Huis in 't Veld, P.J., Mechtler, K., and Peters, J.M. (2013). Aurora B and Cdk1 mediate Wapl activation and release of acetylated cohesin from chromosomes by phosphorylating Sororin. *Proc. Natl. Acad. Sci. USA* **110**, 13404–13409.
- O'Donovan, D.J., Stokes-Rees, I., Nam, Y., Blacklow, S.C., Schröder, G.F., Brunger, A.T., and Sliz, P. (2012). A grid-enabled web service for low-resolution crystal structure refinement. *Acta Crystallogr. D Biol. Crystallogr.* **68**, 261–267.
- Ouyang, Z., Zheng, G., Song, J., Borek, D.M., Otwinowski, Z., Brautigam, C.A., Tomchick, D.R., Rankin, S., and Yu, H. (2013). Structure of the human cohesin inhibitor Wapl. *Proc. Natl. Acad. Sci. USA* **110**, 11355–11360.
- Panizza, S., Tanaka, T., Hochwagen, A., Eisenhaber, F., and Nasmyth, K. (2000). Pds5 cooperates with cohesin in maintaining sister chromatid cohesion. *Curr. Biol.* **10**, 1557–1564.
- Parelho, V., Hadjir, S., Spivakov, M., Leleu, M., Sauer, S., Gregson, H.C., Jarmuz, A., Canzonetta, C., Webster, Z., Nesterova, T., et al. (2008). Cohesins functionally associate with CTCF on mammalian chromosome arms. *Cell* **132**, 422–433.
- Pernot, P., Round, A., Barrett, R., De Maria Antolinos, A., Gobbo, A., Gordon, E., Huet, J., Kieffer, J., Lentini, M., Mattenet, M., et al. (2013). Upgraded ESRF BM29 beamline for SAXS on macromolecules in solution. *J. Synchrotron Radiat.* **20**, 660–664.
- Peters, J.-M., and Nishiyama, T. (2012). Sister chromatid cohesion. *Cold Spring Harb. Perspect. Biol.* **4**, a011130.
- Petoukhov, M.V., Franke, D., Shkumatov, A.V., Tria, G., Kikhney, A.G., Gajda, M., Gorba, C., Mertens, H.D., Konarev, P.V., and Svergun, D.I. (2012). New developments in the ATSAS program package for small-angle scattering data analysis. *J. Appl. Cryst.* **45**, 342–350.
- Roig, M.B., Löwe, J., Chan, K.L., Beckouët, F., Metson, J., and Nasmyth, K. (2014). Structure and function of cohesin's Scc3/SA regulatory subunit. *FEBS Lett.* **588**, 3692–3702.
- Rolf Ben-Shahar, T., Heeger, S., Lehane, C., East, P., Flynn, H., Skehel, M., and Uhlmann, F. (2008). Eco1-dependent cohesin acetylation during establishment of sister chromatid cohesion. *Science* **321**, 563–566.
- Rowland, B.D., Roig, M.B., Nishino, T., Kurze, A., Uluocak, P., Mishra, A., Beckouët, F., Underwood, P., Metson, J., Imre, R., et al. (2009). Building sister chromatid cohesion: smc3 acetylation counteracts an antiestablishment activity. *Mol. Cell* **33**, 763–774.

- Schröder, G.F., Levitt, M., and Brunger, A.T. (2010). Super-resolution bi-molecular crystallography with low-resolution data. *Nature* **464**, 1218–1222.
- Schrodinger, LLC (2010). *The PyMOL Molecular Graphics System, Version 1.3r1*.
- Shintomi, K., and Hirano, T. (2009). Releasing cohesin from chromosome arms in early mitosis: opposing actions of Wapl-Pds5 and Sgo1. *Genes Dev.* **23**, 2224–2236.
- Sjögren, C., and Nasmyth, K. (2001). Sister chromatid cohesion is required for postreplicative double-strand break repair in *Saccharomyces cerevisiae*. *Curr. Biol.* **11**, 991–995.
- Stead, K., Aguilar, C., Hartman, T., Drexel, M., Meluh, P., and Guacci, V. (2003). Pds5p regulates the maintenance of sister chromatid cohesion and is sumoylated to promote the dissolution of cohesion. *J. Cell Biol.* **163**, 729–741.
- Sumara, I., Vorlaufer, E., Gieffers, C., Peters, B.H., and Peters, J.M. (2000). Characterization of vertebrate cohesin complexes and their regulation in prophase. *J. Cell Biol.* **151**, 749–762.
- Sutani, T., Kawaguchi, T., Kanno, R., Itoh, T., and Shirahige, K. (2009). Budding yeast Wpl1(Rad61)-Pds5 complex counteracts sister chromatid cohesion-establishing reaction. *Curr. Biol.* **19**, 492–497.
- Svensson, O., Malbet-Monaco, S., Popov, A., Nurizzo, D., and Bowler, M.W. (2015). Fully automatic characterization and data collection from crystals of biological macromolecules. *Acta Crystallogr. D Biol. Crystallogr.* **71**, 1757–1767.
- Tanaka, K., Hao, Z., Kai, M., and Okayama, H. (2001). Establishment and maintenance of sister chromatid cohesion in fission yeast by a unique mechanism. *EMBO J.* **20**, 5779–5790.
- Tedeschi, A., Wutz, G., Huet, S., Jaritz, M., Wuensche, A., Schirghuber, E., Davidson, I.F., Tang, W., Cisneros, D.A., Bhaskara, V., et al. (2013). Wapl is an essential regulator of chromatin structure and chromosome segregation. *Nature* **501**, 564–568.
- Unal, E., Heidinger-Pauli, J.M., Kim, W., Guacci, V., Onn, I., Gygi, S.P., and Koshland, D.E. (2008). A molecular determinant for the establishment of sister chromatid cohesion. *Science* **321**, 566–569.
- Vaur, S., Feytout, A., Vazquez, S., and Javerzat, J.P. (2012). Pds5 promotes cohesin acetylation and stable cohesin-chromosome interaction. *EMBO Rep.* **13**, 645–652.
- Winn, M.D., Ballard, C.C., Cowtan, K.D., Dodson, E.J., Emsley, P., Evans, P.R., Keegan, R.M., Krissinel, E.B., Leslie, A.G., McCoy, A., et al. (2011). Overview of the CCP4 suite and current developments. *Acta Crystallogr. D Biol. Crystallogr.* **67**, 235–242.
- Yan, J., Enge, M., Whittington, T., Dave, K., Liu, J., Sur, I., Schmierer, B., Jolma, A., Kivioja, T., Taipale, M., and Taipale, J. (2013). Transcription factor binding in human cells occurs in dense clusters formed around cohesin anchor sites. *Cell* **154**, 801–813.
- Zhang, J., Shi, X., Li, Y., Kim, B.J., Jia, J., Huang, Z., Yang, T., Fu, X., Jung, S.Y., Wang, Y., et al. (2008). Acetylation of Smc3 by Eco1 is required for S phase sister chromatid cohesion in both human and yeast. *Mol. Cell* **31**, 143–151.